

Decoupled Smith predictor for multivariable nonsquare systems with multiple time delays

A. SESHAGIRI RAO AND M. CHIDAMBARAM*

Department of Chemical Engineering, Indian Institute of Technology Madras, Chennai 600 036, India.
email: chidam@iitm.ac.in; Phone: 044-2257 4155; Fax: 044-2257 0509.

Received on June 23, 2005; Revised on February 8, 2006.

Abstract

The classical multivariable Smith predictor is extended to multivariable nonsquare systems with multiple time delays where the number of process inputs is higher than the process outputs. Pairing for input and output variables is carried out using the block relative gain technique. Simplified decoupling method is applied to design the decouplers. The decoupled processes are modeled as first-order plus time-delay model or second-order plus time-delay model with positive/negative zero. The controllers are designed individually based on the identified models. For the delay-compensated system, decentralized multivariable proportional-integral controllers are designed by internal model control method for FOPTD models. To show the improvement, PI controllers for the uncompensated system are also designed by simplified internal model control method. For SOPTD models, a method similar to Chien *et al.* [Simple PID controller tuning method for processes with inverse response plus dead time or large overshoot response plus dead time, *Ind. Eng. Chem. Res.*, **42**, 4461–4477 (2003)] is proposed for controller design in the delay compensator. The proposed method is applied to shell standard control problem (3 input and 2 output), hot oil fractionator (4 input and 2 output) and mixing tank (3 input and 2 output). Simulation studies were carried out for both servo and regulatory problems. Robustness studies were carried out for uncertainty in all the process model parameters. It is shown that the performance of the multivariable delay-compensated system with decentralized PI controllers is significantly better than that of the multivariable control system without any delay compensator.

Keywords: Smith predictor, nonsquare systems, decentralized controller, block relative gain.

1. Introduction

Time delays occur frequently in process control loops due to distance velocity lags, recycle loops, delay in measurements, etc. The principal difficulty with the time-delay systems is in the increased phase lag, which limits the possible amount of control action. The complication involved with the time delays further increases in multivariable systems due to the multivariable nature, where different time delays are present in different control loops and due to interactions. In 1957, Smith [1] first designed a delay compensator for single-input single-output (SISO) time-delay processes. The inclusion of dead time compensator removes the delay from the characteristic equation thereby allowing increased value for controller gain. Alevisakis and Seborg [2, 3] have extended the original Smith delay compensator to multi-input multi-output (MIMO) processes with equal time delay. Ogunnaike and Ray [4]

*Author for correspondence.

have extended it to MIMO processes with multiple time delays. Jerome and Ray [5] have proposed a multidelay compensator in which both time delay and interaction compensation were achieved within a single design.

Wang *et al.* [6] have proposed a decoupled Smith delay compensator for MIMO processes with multiple time delays, where they have used frequency domain approach for the decoupler design. Later, Wang *et al.* [7] have designed the decoupling controller for MIMO processes with multiple time delays using the IMC framework. Reddy *et al.* [8] have shown that using Davison's method [9] one can get better control system performance for stable and non-minimum phase systems compared to Wang *et al.* [7]. The Davison's method is simple to design, whereas that of Wang *et al.* [7] is complicated in designing controllers. As the original Smith delay compensator is sensitive for model uncertainties, it is recommended [10] to use a first-order filter on the estimated load effects to increase the robustness for SISO processes. The work so far discussed is concerned about the MIMO square systems.

Processes with equal number of inputs and outputs are known as square systems whereas those with unequal numbers are known as nonsquare systems. The systems with more outputs than inputs are generally not desirable as all of the outputs cannot be maintained at the set point since the system is undermined. Systems with more inputs than outputs are frequently encountered in process industries. Some examples of nonsquare systems with time delays are: Shell control problem [11], with three manipulated variables and two controlled variables, hot oil fractionator [12] with four manipulated variables and two controlled variables, and mixing tank problem with three manipulated variables and two controlled variables [13]. One technique to control such nonsquare systems is by squaring down the system and designing the decentralized multivariable controllers, but it results in poor performance because of the information neglected by its structure [9].

Loh and Chiu [14] have shown that nonsquare systems should be controlled in their original state instead of squaring down by adding or deleting the variables. So designing the controllers for nonsquare systems gives an improved practical insight. Recently, Sharma and Chidambaram [15] have proposed a method to control nonsquare systems using Davison's method [9] to design centralized controllers. They have extended the design method of Davison [9] to nonsquare systems by taking pseudo-inverse to the steady-state process gain matrix, and have used Routh–Hurwitz stability criteria to find the range of controller tuning parameters. Minimum ISE technique is used to find out the final tuning parameters. As the characteristic equation contains time delay term, there is a limit on controller gain and thereby limit the possible amount of control action for delay dominant processes. Also with centralized controllers, the interaction effects will be severe compared to that of the decoupled controllers.

To enhance the control system performance, a delay compensation technique should be used in these conditions. In the present work, multivariable Smith delay compensator with decoupler is applied by simulation to multivariable nonsquare systems with multiple time delays. Simulation applications to Shell standard control problem, fractionator problem and mixing tank problem are given.

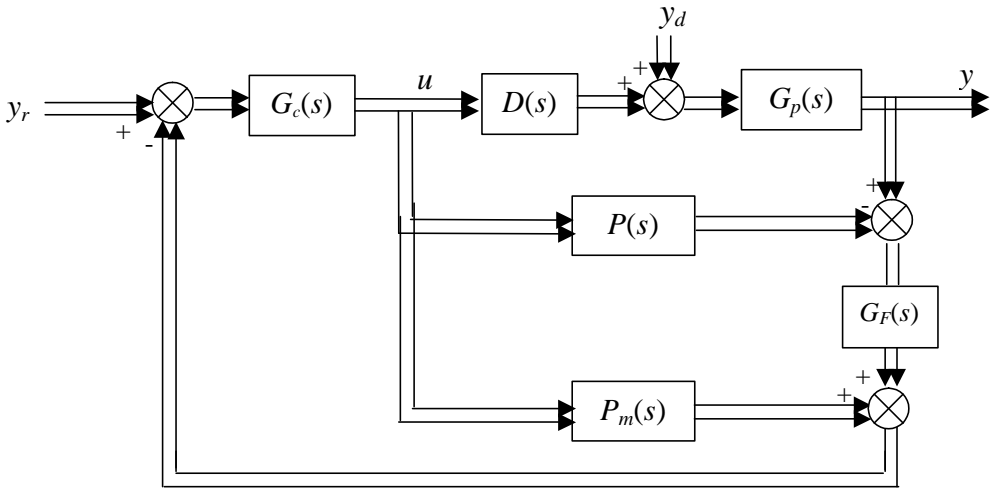


FIG. 1. Decoupled Smith delay compensator for MIMO nonsquare processes with filter.

2. Methodology

The control block diagram of Smith delay compensator applied to multivariable nonsquare system is shown in Fig. 1, where G_p is the transfer function matrix of the process with m inputs and n outputs, G_c is the transfer function matrix of the controller with m outputs and n inputs where $m > n$. G_F is the filter transfer function matrix (size: $n \times n$) with first-order filters for each controlled variable. D is the transfer function matrix of the decoupler of size $[m \times m]$ in which the diagonal elements are equal to one. The block diagram without any delay compensator is shown in Fig. 2. The MIMO transfer function matrix for G_p is considered as

$$G_{p,n \times m}(s) = \begin{bmatrix} G_{11} & G_{12} & \dots & \dots & G_{1m} \\ G_{21} & G_{22} & \dots & \dots & \dots \\ \dots & \dots & \dots & \dots & \dots \\ \dots & \dots & \dots & \dots & \dots \\ G_{n1} & \dots & \dots & \dots & G_{nm} \end{bmatrix}. \tag{1}$$

The decoupler matrix for m manipulated variables is considered as

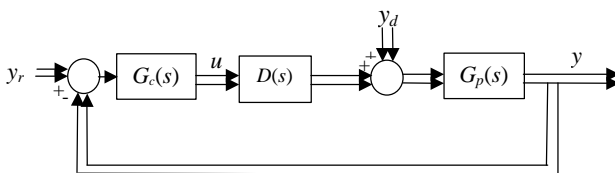


FIG. 2. MIMO feedback structure without delay compensator.

$$D_{m \times m}(s) = \begin{bmatrix} D_{11} & D_{12} & \dots & \dots & D_{1m} \\ D_{21} & D_{22} & \dots & \dots & \dots \\ \dots & \dots & \dots & \dots & \dots \\ \dots & \dots & \dots & \dots & \dots \\ D_{m1} & \dots & \dots & \dots & D_{mm} \end{bmatrix}, \quad (2)$$

where the diagonal elements $D_{11} = D_{22} = \dots = D_{mm} = 1$. Based on the pairing of the output variables to the input variables, the remaining decouplers are designed. Correspondingly, the controller matrix for the decoupled model ($G_p D$) is considered as

$$G_{c, m \times n}(s) = \begin{bmatrix} G_{c11} & G_{c12} & \dots & \dots & G_{c1n} \\ G_{c21} & G_{c22} & \dots & \dots & \dots \\ \dots & \dots & \dots & \dots & \dots \\ \dots & \dots & \dots & \dots & \dots \\ G_{c,m1} & \dots & \dots & \dots & G_{c,mn} \end{bmatrix}. \quad (3)$$

The controllers are designed based on decoupled model individually. In Fig. 1, P_m is the decoupled process model without time delay, and P is the decoupled process model with time delay.

3. Decoupler design

For the given MIMO nonsquare process, G_p , block relative gain (BRG) method [13] is used for pairing of the controlled variables to the manipulated variables, after which simplified decoupling is applied to design the decouplers. The decoupled process (process G_p along with the decouplers) is modeled either as FOPTD or SOPTD model with a positive/negative zero. If the decoupled process shows a first-order response behavior, then simple process reaction curve (PRC) method is used to identify the decoupled process as FOPTD model, i.e. in the form of $K_p e^{-qs}/(\tau s + 1)$. If the decoupled process shows slightly inverse response characteristics, then also the decoupled process is approximated with PRC method to FOPTD model.

However, when there are large inverse response characteristics in the decoupled process, modeling as an FOPTD using PRC method is not adequate. Hence, for these types of processes, least squares (LS) optimization method is chosen to identify the models as SOPTD with positive zero, i.e. in the form of $K_p(1 - ps)e^{-qs}/(\tau_1 s + 1)(\tau_2 s + 1)$. If the decoupled process shows a quick response with high overshoot, then the model is identified as $K_p(1 + ps)e^{-qs}/(\tau_1 s + 1)(\tau_2 s + 1)$. LS method is simple to use here because the time delay (q) and the process gain (K_p) are known from the original decoupled process. Only the time constants (τ_1 and τ_2) and the model zero (p) values need to be calculated. The initial guess for these values can be easily obtained from the original decoupled process response.

3.1. Remarks in decoupler design

If a nonrealizable part in the decoupler (example, positive time delay) occurs in deriving the decouplers, those terms are neglected in the decoupler design, but it will lead to some inter-

action. To avoid this type of problem, a delay matrix can be introduced to make the decoupler matrix realizable. Ogunnaike and Ray [12] have shown that for MIMO square systems, the nonrealizable part due to time delay can be neglected by having small time delays in the diagonal processes compared to other processes. The same technique can be applied to MIMO nonsquare systems also, but incorporating an additional delay matrix delays the overall performance of the control system further. Hence, there is a tradeoff for getting the no interaction responses and the performance. If the demand is perfect decoupling, then the delay matrix should be introduced. Otherwise, the terms leading to nonrealizable parts can be neglected (Appendix I).

4. Controller design

Based on the decoupled process model, the decentralized controllers are designed individually. As the design of the controllers in the Smith predictor is based on the model without any time delay, the controllers are designed based on the model only without considering time delay. For the uncompensated system, the controllers are designed based on the model with time delay. For the three types of models identified, the controller design methods are explained below.

4.1. Case (i)

The identified model is

$$G_m(s) = k_m e^{-qs} / (ts + 1). \quad (4)$$

Here, simplified internal model control (SIMC) method proposed by Skogestad [16] is used for the PI controller design. The controller settings for the model with time delay are $k_c = \mathbf{t}_m / k_m (\mathbf{t}_c + \mathbf{q})$ and $\mathbf{t}_1 = \min\{\mathbf{t}_m, 4(\mathbf{t}_c + \mathbf{q})\}$, where \mathbf{t}_c is the tuning parameter. As there will be a tradeoff between nominal and robust performances, the tuning parameter has to be selected properly. Skogestad [16] has suggested that the tuning parameter \mathbf{t}_c can be considered as equal to the model time delay (\mathbf{q}) for good nominal and robust performances. IMC method is used of the controller design for the model without time delay for the Smith predictor. The controller settings are given by $k_c = \mathbf{t}_m / k_m \mathbf{t}_s$ and $\mathbf{t}_1 = \min\{\mathbf{t}_m, 4\mathbf{t}_s\}$, where \mathbf{t}_s is the tuning parameter. The tuning parameter is to be selected to ensure that both nominal as well as robust performances are obtained. For this, it is observed that τ_s can be taken around $\mathbf{q}/2$.

4.2. Case (ii)

The model identified is

$$G_m(s) = k_m (1 - ps) e^{-qs} / (\mathbf{t}_1 s + 1)(\mathbf{t}_2 s + 1). \quad (5)$$

Here, the design method of Chien *et al.* [17] is adopted for the controller design of the model with time delay. The controller settings are given by $k_c = \tau_1 / k_m (2\mathbf{t}_{c1} + \mathbf{q} + p)$, $\mathbf{t}_1 = \mathbf{t}_1$ and $\mathbf{t}_D = \mathbf{t}_2$, where \mathbf{t}_{c1} is given as $\mathbf{t}_{c1} = 0.1\mathbf{q} + 0.5\sqrt{4p\mathbf{q} + 0.4p\mathbf{t}_D + 0.4\theta\mathbf{t}_D + 0.04\mathbf{t}_D^2}$. Chien *et al.* [17] have suggested that the PID controller should be implemented in the form of

$$k_c \left(1 + \frac{1}{\mathbf{t}_I s} \right) \left[y_i^{sp} - \frac{(\mathbf{t}_D s + 1)}{(0.1 \mathbf{t}_D s + 1)} y_i \right], i = 1, 2,$$

to avoid the derivative kick. Hence, in the present work, the controllers are implemented in the same form.

As a simple PI controller gives good performance in the Smith predictor, in the present work, only PI controller is used in the Smith predictor. The design procedure of the PID controller is adopted from Chien *et al.* [17] and is briefly explained here. The process model considered is eqn (5) without time delay. Let us consider the PI controller as

$$G_c = k_c \left(1 + \frac{1}{\mathbf{t}_I s} \right).$$

The closed loop characteristic equation becomes $1 + G_c G_m = 0$. By considering $\mathbf{t}_1 = \mathbf{t}_1$, the resulting closed loop characteristic equation is given by

$$\left(\frac{\mathbf{t}_1 \mathbf{t}_2}{k_c k_m} \right) s^2 + \left(\frac{\mathbf{t}_1 - k_c k_m p}{k_c k_m} \right) s + 1 = 0.$$

The equation is set to match a desired critically damped closed loop characteristic equation such as $\mathbf{t}_{cl}^2 s^2 + 2\mathbf{t}_{cl} s + 1 = 0$. By equating the corresponding coefficients the controller gain is obtained as $k_c = (\mathbf{t}_{cl} \mathbf{t}_1 - 2\mathbf{t}_1 \mathbf{t}_2) / (k_m \mathbf{t}_{cl} p)$, where \mathbf{t}_{cl} is the desired closed-loop time constant. \mathbf{t}_{cl} has to be selected such that both nominal and robust performances are achieved. \mathbf{t}_{cl} has to be selected to satisfy the constraint $\mathbf{t}_{cl} > 2\mathbf{t}_2$.

4.3. Case (iii)

The model identified is

$$G_m(s) = k_m (1 + ps) e^{-qs} / (\mathbf{t}_1 s + 1)(\mathbf{t}_2 s + 1). \quad (6)$$

The design procedure is the same as explained in Case (ii), and the resulting controller settings are $k_c = (2\mathbf{t}_1 \mathbf{t}_2 - \mathbf{t}_{cl} \mathbf{t}_1) / (k_m \mathbf{t}_{cl} p)$ and $\mathbf{t}_1 = \mathbf{t}_1$. Here the tuning parameter (\mathbf{t}_{cl}) has to be selected in such a way that it satisfies the constraint $\mathbf{t}_{cl} < 2\mathbf{t}_2$.

4.4. Selecting the filter constants in the Smith predictor

The value of filter time constant is considered as equal to the time delay of the corresponding model if there are small perturbations in the individual process parameters. If the controlled variable is paired with two or more manipulated variables, the filter constant is considered as equal to the largest time delay of the corresponding decoupled model. If the uncertainties in the process parameters are large, then the filter constant can be taken as greater than two times the corresponding time delay.

5. Robustness of decoupled Smith predictor

The designed control system should meet the disturbance attenuation, set point tracking, robust stability and robust performance besides nominal stability. Disturbance attenuation is

achieved when the norm of the transfer function matrix from the disturbance (y_d) to the output (y) is made small. Similarly, set point tracking is achieved when the norm of the transfer function matrix from the set point (y_r) to the error (e) is made small.

The multivariable Smith predictor configuration (Fig. 1) is referred to as the nominal case if $G_p D = P$. As the process G_p is assumed to be stable and the decoupler D is designed to be stable, the control system in Fig. 1 will be stable if and only if the primary controller G_c stabilizes P_m . The nominal condition $G_p D = P$ can be violated in practice due to the following reasons. Firstly, due to the approximation of the decoupler by model reduction, the transfer matrix $G_p D$ may not be diagonal, whereas P is implemented as diagonal form. Most importantly, in the real world, the model G_p may not represent the actual process exactly. For robustness analysis, the actual process is assumed to be any member of a family of possible processes.

Typically, the three types of uncertainties, which are most commonly encountered in practice and require to be pertinently coped with during the system operation are additive, multiplicative input and multiplicative output uncertainties [18]. Smith predictor system with the process additive uncertainties is shown in Fig. 3. The additive uncertainties can be regarded as parameter perturbation of the process transfer function matrix and describe the actual process family as

$$\Pi = \{G(s):G(s) = G_p(s) + \Delta_A(s)\}, \tag{7}$$

where $\Delta_A(s)$ is the additive uncertainty and is assumed to be stable. $G_p(s)$ is the nominal process transfer function matrix and $G(s)$, the actual process transfer function matrix. Hence, the uncertainty matrix is $\Delta_A(s) = G(s) - G_p(s)$. From Fig. 3, the transfer function matrix from the inputs () to the outputs (v) of $\Delta A(s)$ is obtained as

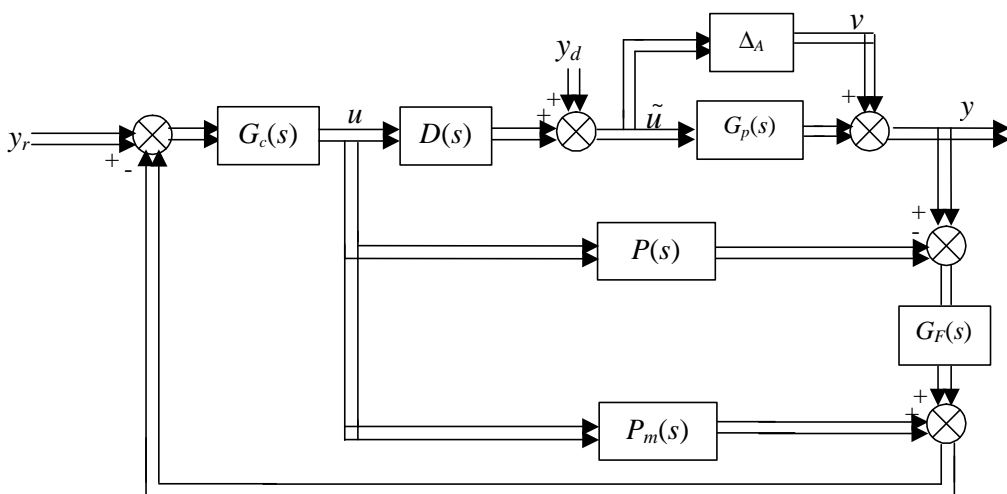


FIG. 3. Decoupled Smith delay compensator for MIMO nonsquare processes with additive uncertainty (Δ_A).

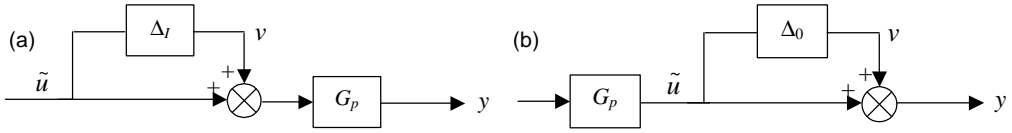


FIG. 4. (a) Input multiplicative uncertainty; (b) Output multiplicative uncertainty.

$$H_A(s) = -DG_c G_F [I + G_F G_p DG_c - (G_F P - P_m) G_C]^{-1}. \quad (8)$$

According to the small gain theorem the closed-loop system is robustly stable if and only if [19]

$$\tilde{\mathbf{s}}[H_A(s)] < \frac{1}{\tilde{\mathbf{s}}[\Delta_A(s)]} \quad (9)$$

where $\tilde{\mathbf{s}}(\cdot)$ is the maximum singular value. Similar rule applies when there exists process input uncertainty or process output uncertainty. The process input and output uncertainties without the Smith predictor structure are shown in Figs 4(a) and (b), respectively. From these figures, according to the small gain theorem, the robust stability is satisfied if and only if [19]

$$\tilde{\mathbf{s}}[H_I(s)] < \frac{1}{\tilde{\mathbf{s}}[\Delta_I(s)]} \quad (10a)$$

$$\tilde{\mathbf{s}}[H_o(s)] < \frac{1}{\tilde{\mathbf{s}}[\Delta_o(s)]} \quad (10b)$$

where H_I and H_o are the relations from the input () to the output (v) of the uncertainties as shown in Fig. 4(a) and (b). Here, Δ_I is the input uncertainty and Δ_o is the output uncertainty and both Δ_I and Δ_o are considered stable.

The maximum and minimum singular values [$\tilde{\mathbf{s}}(\cdot)$ and $\underline{\mathbf{s}}(\cdot)$] of the sensitivity and complementary sensitivity functions are also measures of the robustness of any closed-loop control system [19, 20]. Quick set point tracking and low-frequency disturbance rejection are ensured if the maximum singular values of the sensitivity function are low at low frequencies and minimum singular values of the complementary sensitivity function are high at low frequencies. In addition, the peak value of the maximum singular values of the complementary sensitivity function should be low to get less oscillatory responses for model mismatches.

6. Simulation studies

For the purpose of simulation three case studies are considered.

6.1. Case study 1

The process considered is a Shell control problem [11] with two controlled variables and three manipulated variables in which the two controlled variables are composition of the

top product and that of side stream. The manipulated variables are top draw, side draw and the bottoms reflux. As the delay compensator is significant for delay dominant processes, here the time delays are considered as five times to the time constants of each transfer function in the process. The resulting process is given by:

$$G_p(s) = \begin{bmatrix} \frac{4.05e^{-250s}}{50s+1} & \frac{1.77e^{-300s}}{60s+1} & \frac{5.88e^{-250s}}{50s+1} \\ \frac{5.39e^{-250s}}{50s+1} & \frac{5.72e^{-300s}}{60s+1} & \frac{6.9e^{-200s}}{40s+1} \end{bmatrix}. \quad (11)$$

The steady-state gains for the process are

$$G_p(s) = \begin{bmatrix} 4.05 & 1.77 & 5.88 \\ 5.39 & 5.72 & 6.9 \end{bmatrix}. \quad (12)$$

For the 2×3 process, the decoupler and the controller matrices are given by

$$D_{3 \times 3} = \begin{bmatrix} D_{11} & D_{12} & D_{13} \\ D_{21} & D_{22} & D_{23} \\ D_{31} & D_{32} & D_{33} \end{bmatrix}, \quad (13)$$

$$G_{c_{3 \times 2}} = \begin{bmatrix} G_{c11} & G_{c12} \\ G_{c21} & G_{c22} \\ G_{c31} & G_{c32} \end{bmatrix}, \quad (14)$$

where G_c is a matrix of PI controllers. The concept of BRG is applied to eqn (8). The definition and method of calculating BRG are given in Reeves and Arkun [13]. From BRG, it is noted that y_1 is paired with u_1 and u_3 and y_2 is paired with u_2 . The resulting equations for the controlled variables are given by:

$$y_1 = [G_{11} + G_{12}D_{21}]v_1 + [G_{13} + G_{12}D_{23}]v_3 \quad (15a)$$

$$y_2 = [G_{22} + G_{21}D_{12}]v_2 \quad (15b)$$

where the decouplers are given by $D_{11} = D_{22} = D_{33} = 1$, $D_{12} = -G_{12}/G_{11}$, $D_{23} = -G_{23}/G_{22}$, $D_{21} = -G_{21}/G_{22}$ and the remaining decouplers equal zero. The detailed control block diagram with the decouplers without the delay compensator is shown in Fig. 5. The decoupled processes are $P_1 = G_{11} + G_{12}D_{21}$, $P_3 = G_{13} + G_{12}D_{23}$, $P_2 = G_{22} + G_{21}D_{12}$. As the nature of the decoupled processes is of first order, these are identified as FOPTD models using PRC method. The identified models are given by:

$$P_1 = 2.383e^{-250s}/(23.25s + 1), P_3 = 3.744e^{-250s}/(25.747s + 1), P_2 = 3.365e^{-300s}/(59.98s + 1).$$

Based on these models, the decentralized controllers are designed independently (G_{c11} based on P_1 , G_{c31} based on P_3 and G_{c22} based on P_2) using the SIMC method [16]. The controllers designed without the compensator are:

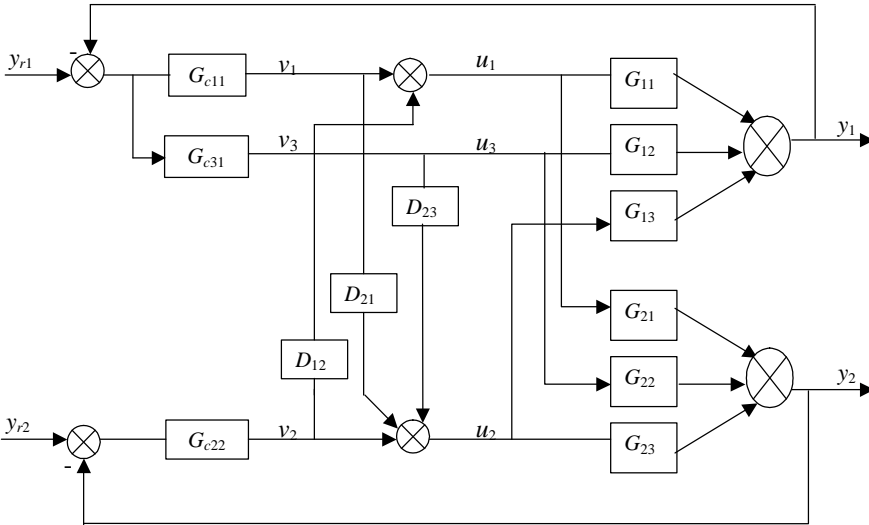


FIG. 5. MIMO nonsquare control block diagram without delay compensator for case study-1.

$$G_{c11} : K_c = 9.756/(\mathbf{t}_{c11} + 250), \mathbf{t}_1 = 23.25 \tag{16a}$$

$$G_{c31} : K_c = 6.876/(\mathbf{t}_{c31} + 250), \mathbf{t}_1 = 25.747 \tag{16b}$$

$$G_{c22} : K_c = 17.824/(\mathbf{t}_{c22} + 300), \mathbf{t}_1 = 59.98 \tag{16c}$$

where \mathbf{t}_{cij} is the tuning parameter. Skogestad [16] has suggested that the tuning parameter could be taken as equal to the time delay for good nominal and robust performances. Thus the controller matrix is obtained as

$$G_{c_{3 \times 2}} = \begin{bmatrix} 0.0195 + \frac{0.00084}{s} & 0 \\ 0 & 0.0297 + \frac{0.00055}{s} \\ 0.0137 + \frac{0.00053}{s} & 0 \end{bmatrix}. \tag{17}$$

As explained in Section 4.1, the controllers are designed for the delay-compensated system without considering the time delay term. The tuning parameter is selected as half of the time delay. Hence, the controllers are obtained as

$$G_{c_{3 \times 2}} = \begin{bmatrix} 0.078 + \frac{0.00335}{s} & 0 \\ 0 & 0.118 + \frac{0.002}{s} \\ 0.055 + \frac{0.00213}{s} & 0 \end{bmatrix}. \tag{18}$$

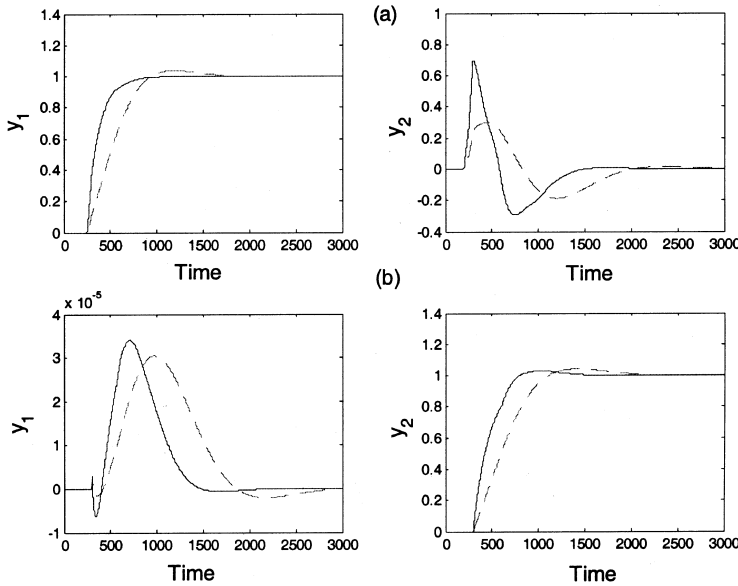


FIG. 6. Comparison of servo responses for perfect model for case study-1; step change in (a) y_{r1} , and (b) y_{r2} . Legend: solid—with delay compensator, dash—without delay compensator.

With these controllers, the performances are evaluated for delay-compensated system and the system without the delay compensator by giving unit step changes in y_{r1} or y_{r2} . Figure 6 shows the responses for servo problem for perfect model parameters and Fig. 7 for the

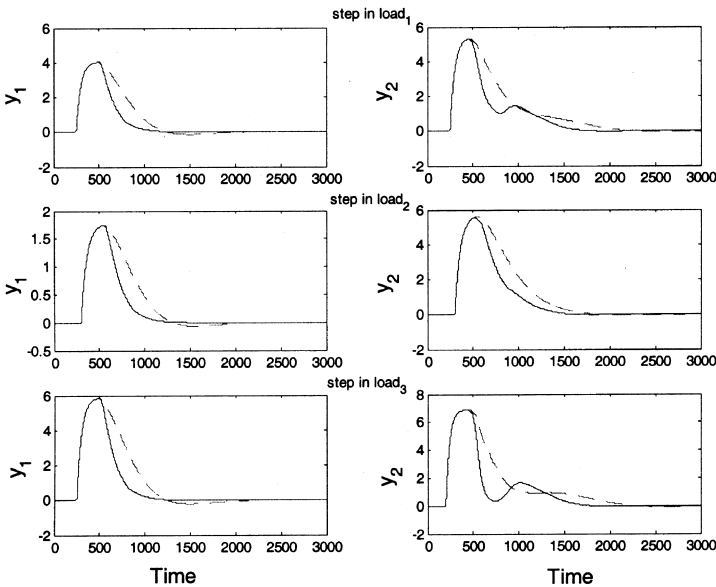


FIG. 7. Comparison of regulatory responses for perfect model for case study-1. Legend: solid—with delay compensator, dash—without delay compensator.

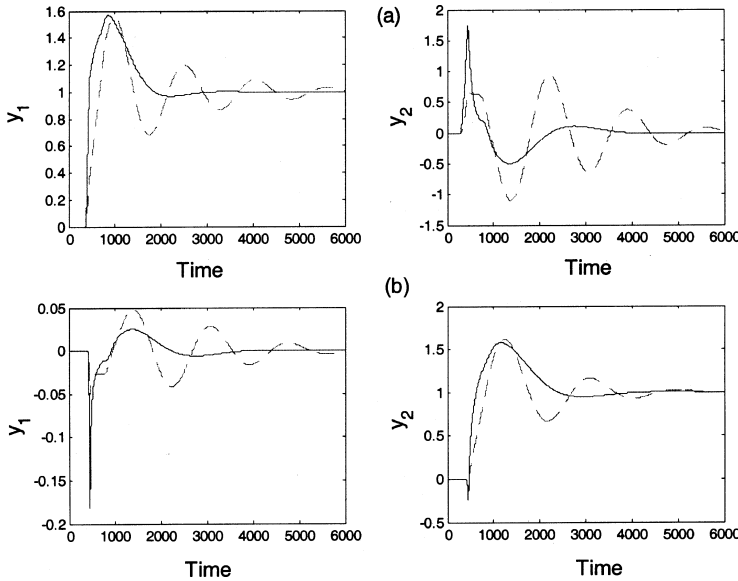


FIG. 8. Servo responses when there is a perturbation of 50% in K_p , q and -50% in t . step changes in (a) y_{r1} , and (b) y_{r2} . Legend: solid—with delay compensator, dash—without delay compensator.

regulatory responses. It is observed from the responses that the delay-compensated system performs significantly better compared to that of the system without compensator. Let us consider that there exist large perturbations in the individual process parameters. To simulate the control system with compensator for large uncertainties ($\pm 50\%$), the filter constants for y_1 and y_2 are taken as three times the time delay of P_1 and P_2 , respectively. Figure 8 shows the servo responses for +50% perturbations in each process gain and time delay, and -50% perturbation in each process time constant. From the responses it is clear that the delay-compensated system performs better.

To show the quantitative improvement of the delay-compensated system over that of un-compensated system, the performance criteria chosen is integral of square error (ISE). The ISE values are measured in each output separately and are added to get the total ISE value for a step input in the set point (for example, y_{r1}). The corresponding ISE values are shown in Table I for both the methods for servo responses. Also shown are the ISE values when

Table I
ISE values for case study-1 for perfect parameters

Step in		ISE for y_1	ISE for y_2	Sum of ISE
y_{r1}	With delay compensator	309.94	89.51	399.45
y_{r2}		4.26×10^{-7}	388.54	388.54
y_{r1}	Without compensator (IMC design)	418.36	47.16	465.52
y_{r2}		5.38×10^{-7}	505.77	505.77
y_{r1}	Without compensator (Z-N design)*	459.97	69.44	529.41
y_{r2}		4.64×10^{-7}	548.45	548.45

*Zeigler-Nichols method for the design of controllers without compensator.

the controllers for uncompensated system are designed based on the Zeigler–Nichols method. From the ISE values, it can be observed that the delay-compensated system has low ISE values in all the cases. The quantitative improvement obtained is around 50% in all the cases. When there are large perturbations in the process parameters, the improvement obtained with the delay-compensated system is further better. Vlachos *et al.* [11] have applied genetic algorithm optimization method to calculate the decentralized PI controllers settings for a two-output and two-input system, but the method is time consuming. In the present work, a simple method is proposed for the nonsquare system which gives good control performance for both the nominal and the model mismatch conditions.

6.2. Case study 2

The process considered is a fractionator problem [12] with two controlled variables and four manipulated variables. Here, the individual time delays are considered as three times that of the original process and the resulting system is given by:

$$G_p = \begin{bmatrix} \frac{4.05e^{-81s}}{50s+1} & \frac{1.77e^{-84s}}{60s+1} & \frac{5.88e^{-81s}}{50s+1} & \frac{1.44e^{-81s}}{40s+1} \\ \frac{4.38e^{-60s}}{33s+1} & \frac{4.42e^{-66s}}{44s+1} & \frac{7.2}{19s+1} & \frac{1.26}{32s+1} \end{bmatrix}. \tag{19}$$

Here the decoupling matrix is of 4×4 and the corresponding controller matrix is of 4×2 . Using the BRG, y_1 is paired with u_1 and u_3 and y_2 is paired with u_2 and u_4 . The resulting equations for the controlled variables are:

$$y_1 = [G_{11} + G_{14}D_{41}]v_1 + [G_{13} + G_{14}D_{43}]v_3 = P_1v_1 + P_3v_3 \tag{20a}$$

$$y_2 = [G_{22} + G_{21}D_{12}]v_2 + [G_{24} + G_{22}D_{14}]v_4 = P_2v_2 + P_4v_4 \tag{20b}$$

where the decouplers are given by $D_{12} = -G_{12}/G_{11}$, $D_{14} = -G_{14}/G_{11}$, $D_{41} = -G_{21}/G_{24}$, $D_{43} = -G_{23}/G_{24}$.

In this case, the decoupled processes (P_1, P_3, P_2 and P_4) show large inverse response behavior: thus, these processes are modeled as SOPTD using LS method as explained previously. The models obtained are

$$P_1 = \frac{-0.982(1-241.3s)e^{-93.236s}}{(31.642s+1)^2}, \quad P_3 = \frac{-2.3475(1+105.673s)e^{-80.974s}}{(55.045s+1)(19.817s+1)},$$

$$P_2 = \frac{2.5102(1-4.067s)e^{-63.274s}}{(44.507s+1)(2.034s+1)}, \quad P_4 = \frac{-0.325(1-302.576s)e^{-10.3s}}{(32.757s+1)^2}.$$

Based on these models, the controllers are designed as explained in Sections 4.2 and 4.3, respectively. The controller parameters obtained for the system without the delay compensator are:

$$G_{c11}: K_c = -0.05, \quad t_I = 31.6426, \quad t_D = 31.6426, \quad t_{c1} = 156.6778 \tag{21a}$$

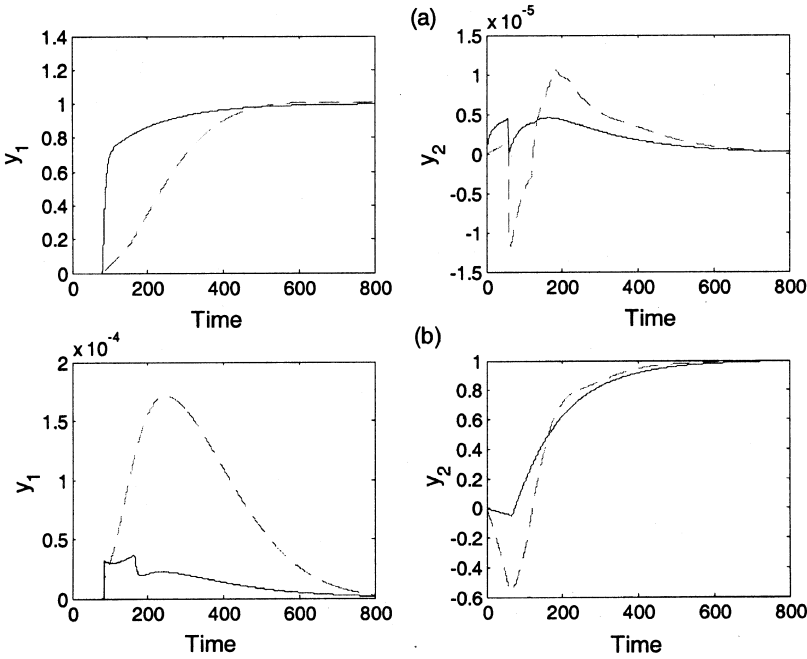


FIG. 9. Comparison servo responses for perfect model for case study-2; step changes in (a) y_{r1} , and (b) y_{r2} . Legend: solid—with delay compensator, dash—without delay compensator.

$$G_{c31}: K_c = -0.1199, t_1 = 55.045, t_D = 19.817, t_{cl} = 57.257; \tag{21b}$$

$$G_{c22}: K_c = 0.1761, t_1 = 44.507, t_D = 2.034, t_{cl} = 16.667; \tag{21c}$$

$$G_{c42}: K_c = -0.2248, t_1 = 32.757, t_D = 32.757, t_{cl} = 67.713. \tag{21d}$$

The controller matrix obtained for the system with compensator is

$$G_{c,4 \times 2} = \begin{bmatrix} -0.0121 - \frac{0.00038}{s} & 0 \\ 0 & 0.3963 + \frac{0.009}{s} \\ -0.6657 - \frac{0.012}{s} & 0 \\ 0 & -0.0302 - \frac{0.00092}{s} \end{bmatrix}. \tag{22}$$

In getting the controllers for the delay-compensated system, the tuning parameters selected are as follows: t_{cl} for case (ii) is considered as $2.2t_2$ (i.e. for P_1, P_2, P_4) and t_{cl} for case (iii) is considered as $t_2/2$ (i.e. for P_3).

With these controller settings, closed-loop performance is evaluated by giving unit step change either in the set point or in the load. Figure 9 shows the responses for the perfect

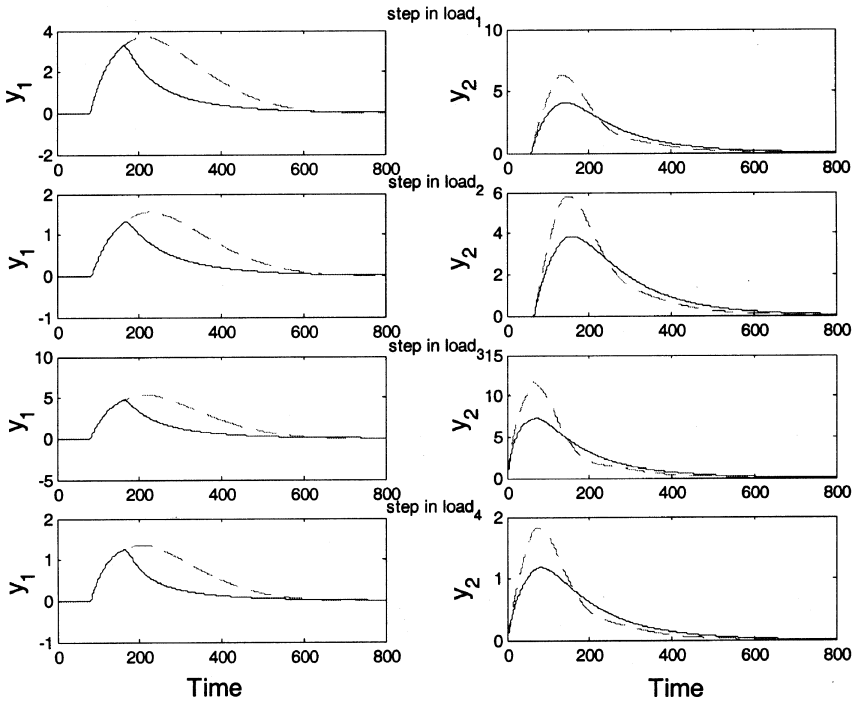


FIG. 10. Comparison of regulatory responses for perfect model of case study-2. Legend: solid—with delay compensator, dash—without delay compensator.

model for set point changes and Fig. 10 for regulatory problem. The responses show that the delay-compensated structure performs significantly better. Figure 11 shows the responses for +30% perturbation in each process gain, time delay and -30% perturbation in each process constant. The filter time constant used for the delay compensator is equal to the corresponding largest time delay for each controlled variable. It is observed that the responses obtained without compensator are completely unstable.

6.3. Case study 3

The process considered is a mixing tank problem with two controlled variables and three manipulated variables [13] in which the two controlled variables are height of liquid in the tank and the exit concentration. The manipulated variables are the flow rates of the three input streams. Time delays are added intentionally to show the improvement of the delay compensator. The resulting process is given in eqn (20).

$$G_p(s) = \begin{bmatrix} \frac{4e^{-100s}}{20s+1} & \frac{4e^{-100s}}{20s+1} & \frac{4e^{-100s}}{20s+1} \\ \frac{3e^{-50s}}{10s+1} & \frac{-3e^{-100s}}{10s+1} & \frac{5e^{-50s}}{10s+1} \end{bmatrix}. \tag{23}$$

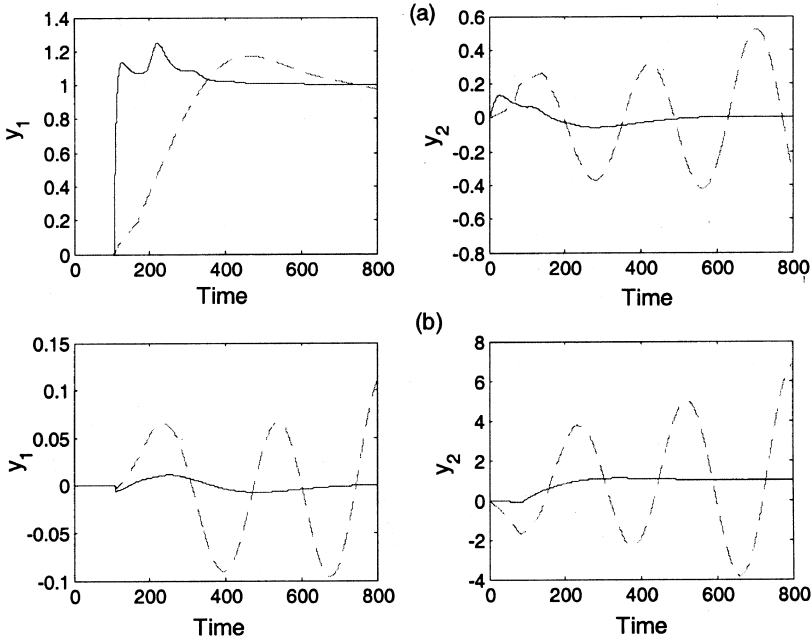


FIG. 11. Servo responses when there is a perturbation of +30% in K_p , q and -30% in t for case study-2; step changes in (a) y_1 , and (b) y_2 . Legend: solid-with delay compensator, dash-without delay compensator.

Using BRG, y_1 is paired with u_1 and u_2 and y_2 is paired with u_3 . The resulting equations for the controlled variables are

$$y_1 = [G_{21} + G_{23}D_{31}]v_1 + [G_{22} + G_{23}D_{32}]v_2; \tag{24a}$$

$$y_2 = [G_{23} + G_{21}D_{13}]v_3, \tag{24b}$$

where the decouplers are given by $D_{13} = -G_{13}/G_{11}$, $D_{31} = -G_{21}/G_{23}$, $D_{32} = -G_{22}/G_{23}$. The decoupled processes are $P_1 = G_{21} + G_{23}D_{31}$, $P_2 = G_{22} + G_{23}D_{32}$, $P_3 = G_{23} + G_{21}D_{13}$. Here, P_1 and P_3 show first-order and P_2 the second-order behavior. Thus P_1 and P_3 are modeled as FOPTD and P_2 as SOPTD with negative zero. The identified models are $P_1 = 1.6e^{-100s}/(20 + 1)$, $P_2 = 1.588(1 + 134.012s)e^{-102s}/(27.412s + 1)^2$, $P_3 = 2e^{-50s}/(10s + 1)$.

Based on these models the decentralized controllers are designed independently. For the design of controllers based on P_1 and P_3 , SIMC method [16] is used. However, for the design of controllers for P_2 , Chien *et al.* [17] method is used. For the design of controller based on P_2 without time delay, the proposed method is used as explained in case (ii) in Section 4. The controllers obtained for the system without any delay compensator are:

$$G_{c11}: K_c = 0.0625, t_1 = 20; \tag{25a}$$

$$G_{c21}: K_c = 0.0701, t_1 = 27.412, t_D = 27.4125, t_F = 134.012, t_{cl} = 72.125; \tag{25b}$$

$$G_{c32}: K_c = 0.005, t_1 = 10. \tag{25c}$$

The controller matrix for the system with delay compensator is obtained as

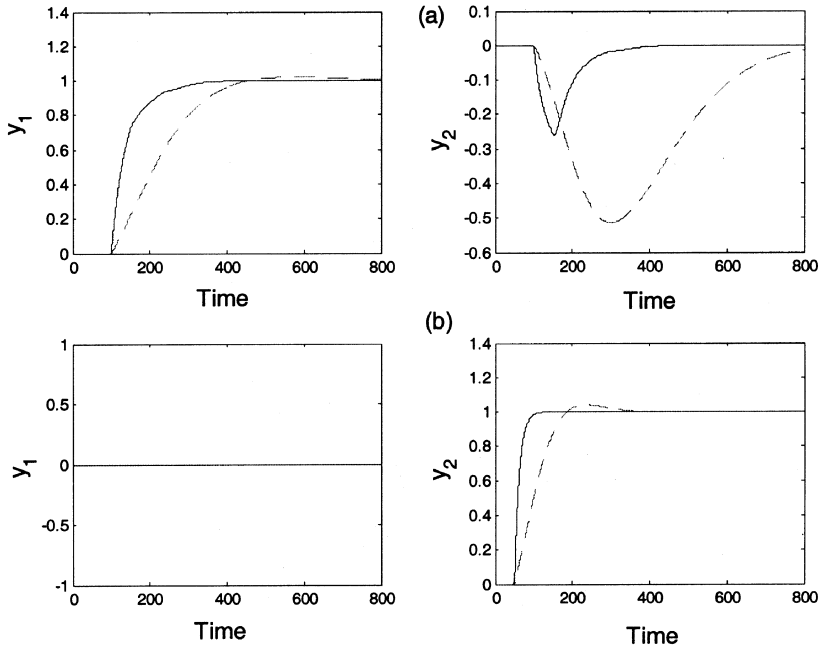


FIG. 12. Comparison of servo responses for perfect model of case study-3; step changes in (a) y_1 , and (b) y_2 . Legend: solid—with delay compensator, dash—without delay compensator.

$$G_{c_{3 \times 2}} = \begin{bmatrix} 0.05 + \frac{0.025}{s} & 0 \\ 0.077 + \frac{0.00281}{s} & 0 \\ 0 & 0.4 + \frac{0.04}{s} \end{bmatrix}. \tag{26}$$

With these controllers, the performances are evaluated for delay-compensated system and the system without the delay compensator by giving unit step change in y_{r1} or y_{r2} . Figure 12 shows the responses for servo problem and Fig. 13 for the regulatory responses for perfect model parameters. From the responses, it is observed that the delay-compensated system performs significantly better compared to that of the system without the compensator.

6.4. Simulation for robustness studies

The maximum and minimum singular values of the sensitivity and complementary sensitivity functions are plotted for mixing tank example for the system with delay and without delay compensation. Figures 14(a) and (b) show, respectively, the maximum and minimum singular values of the sensitivity function and of the complementary sensitivity functions. The maximum singular values of the sensitivity function are low at low frequencies and minimum

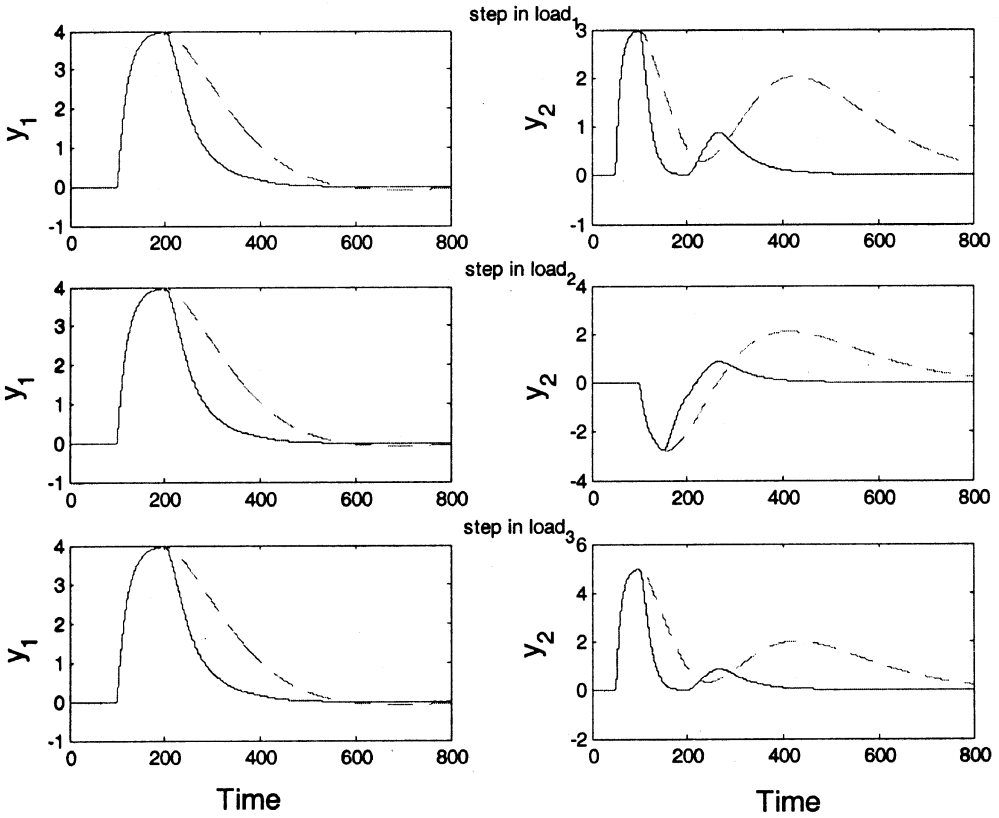


FIG. 13. Comparison of regulatory responses for perfect model of case study-3. Legend: solid—with delay compensator, dash—without delay compensator.

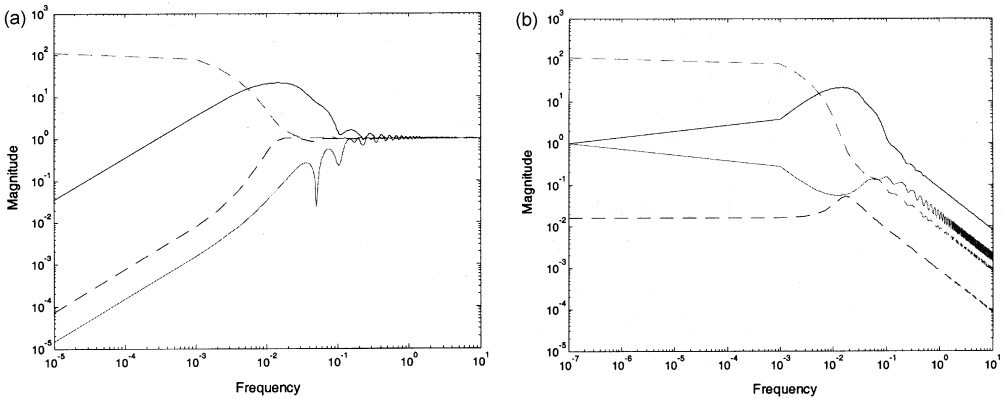


FIG. 14. Maximum and minimum singular values of (a) sensitivity functions, and (b) complementary sensitivity functions. Legend: solid-upper—maximum, solid-lower—minimum for the system with delay compensator; and dash-upper—maximum, dash-lower—minimum singular values for the system without delay compensator.

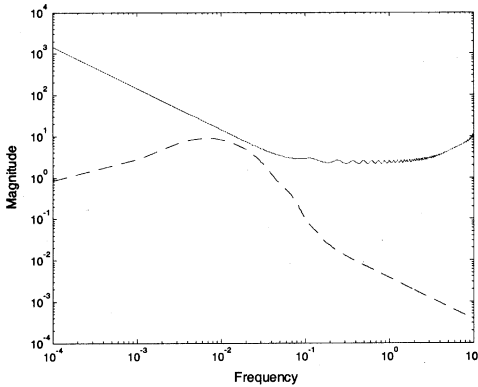


FIG. 15. Robustness to +20% increase in time delays. Legend: solid – $1/\bar{\sigma}[\Delta_A(s)]$, dash – $\bar{\sigma}[H_A(s)]$.

singular values of the complementary sensitivity function are high at low frequencies for the delay-compensated system, when compared with that of the uncompensated system which ensures quick set point tracking and low-frequency disturbance rejection. Also, from Fig. 14(b), it can be observed that the peak value of the maximum singular values of the complementary sensitivity function for the delay-compensated system is less compared to that of the uncompensated system, which shows that less oscillatory responses for model mismatches will result for the delay-compensated system compared to that of the uncompensated system.

Robustness studies were also carried out for additive uncertainties as discussed in Section 5. For the mixing tank problem, a perturbation of +20% in delay is considered in all the nominal process transfer functions (G_p) and hence the additive uncertainty is obtained as $\Delta_A(s) = G(s) - G_p(s)$. Here $G(s)$ is the perturbed model. $\bar{\sigma}[H_A(s)]$ from eqn (8) and $1/\bar{\sigma}[\Delta_A(s)]$ are plotted and are shown in Fig. 15. From the figure it can be observed that the designed controller satisfies the constraint in eqn (9).

7. Conclusions

Smith delay compensator is extended to multivariable nonsquare systems with multiple time delays. Using BRG, the output variables are paired with input variables. The decouplers along with the processes are modeled as FOPTD or SOPTD with positive/negative zero. Based on these decoupled models, controllers are designed independently. If there are large perturbations in the process parameters of the delay compensator, the filter constant can be increased to obtain robust responses. Of the three simulation examples studied, the control system with the delay compensator performs better. Robustness studies carried out by using the maximum and minimum singular values of the sensitivity and complementary sensitivity functions show that the delay-compensated system is more robust than the uncompensated system.

References

1. O. J. M. Smith, Closer control of loops with dead time, *Chem. Engng Prog.*, **53**, 217 (1957).
2. G. Alevisakis, and D. E. Seborg, Extension of Smith delay compensator method to multivariable linear systems containing time delays, *Int. J. Control*, **3**, 541–551 (1973).

3. G. Alevisakis, and D. E. Seborg, Control of multivariable systems containing time delays using a multivariable Smith delay compensator, *Chem. Engng Sci.*, **29**, 373–380 (1974).
4. B. A. Ogunnaike, and W. H. Ray, Multivariable controller design for linear systems having multiple time delays, *AIChE J.*, **25**, 1043 (1979).
5. N. F. Jerome, and W. H. Ray, High performance multivariable control strategies for systems having time delays. *AIChE J.*, **32**, 914–931 (1986).
6. Q. G. Wang, B. Zou, and Y. Zhang, Decoupling Smith delay compensator design for multivariable systems with multiple time delays, *Chem. Engng Res. Des. A*, **78**, 565–572 (2000).
7. Q. G. Wang, Y. Zhang, and M. S. Chiu, Decoupling internal model control for multivariable systems with multiple time delays, *Chem. Engng Sci.*, **57**, 115–124 (2002).
8. P. D. S. Reddy, M. Pandit, and M. Chidambaram, Comparison of multivariable controllers for non-minimum phase systems, *Int. J. Modeling Simulation*, **26**, 4376–4385 (2006).
9. E. J. Davison, Multivariable tuning regulators: The feed forward and robust control of a general servo-mechanism problem. *IEEE Trans. Automatic Control*, **21**, 35–47 (1976).
10. J. E. Normey-Rico, C. Bordón, and E. F. Camacho, Improving the robustness of dead time compensating PI controllers, *Control Engng Practice*, **5**, 801–810 (1997).
11. C. Valchos, D. Williams, and J. B. Gomm, Solution to the shell control problem using genetically tuned PID controllers. *Control Engng Practice*, **10**, 151–163 (2002).
12. B. A. Ogunnaike, and W. H. Ray, *Process dynamics, modeling and control*, Oxford University Press (1992).
13. D. E. Reeves, and Y. Arkun, Interaction measures for non-square decentralized control structure, *AIChE J.*, **35**, 603–613 (1989).
14. E. J. Loh, and M. S. Chiu, Robust decentralized control of non-square systems, *Chem. Engng Commun.*, **158**, 157–180 (1997).
15. K. L. N. Sharma, and M. Chidambaram, Centralized PI/PID controllers for nonsquare systems with RHP zeros, *J. Indian Inst. Sci.*, **85**, 201–221 (2005).
16. S. Skogestad, Simple analytic rules for model reduction and PID controller tuning, *J. Process Control*, **13**, 291–309 (2003).
17. I-Lung Chien, Yu-Cheng Chung, Bo-Shuo Chen, and Cheng-Yuan Chuang, Simple PID controller tuning method for processes with inverse response plus dead time or large overshoot response plus dead time, *Ind. Engng Chem. Res.*, **42**, 4461–4477 (2003).
18. J. C. Doyle, and G. Stein, Multivariable feedback design: concepts for a classical modern synthesis, *IEEE Trans. Automatic Control*, **AC-26**, 4–16 (1981).
19. S. Skogestad, and I. Postlethwaite, *Multivariable feedback control*, Wiley (1996).
20. J. M. Maciejowski, *Multivariable feedback design*, Addison-Wesley (1989).

Appendix A

The tradeoff between perfect decoupling and closed-loop performance is explained here by considering example-1. The process transfer function matrix is given in eqn (11). For this process, after pairing the output and input variables, the decouplers are obtained as $D_{12} = -(G_{12}/G_{11})$, $D_{23} = -(G_{23}/G_{22})$ and $D_{21} = -(G_{21}/G_{22})$. Upon substituting the corresponding

processes, D_{23} and D_{21} result in positive time delay terms that are not realizable. Hence to make the decouplers realizable, according to Ogunnaike and Ray [12], a delay matrix is multiplied to the original process transfer function matrix as

$$G_p(s) = \begin{bmatrix} \frac{4.05e^{-250s}}{50s+1} & \frac{1.77e^{-300s}}{60s+1} & \frac{5.88e^{-250s}}{50s+1} \\ \frac{5.39e^{-250s}}{50s+1} & \frac{5.72e^{-300s}}{60s+1} & \frac{6.9e^{-200s}}{40s+1} \end{bmatrix} \begin{bmatrix} e^{-50s} & 0 & 0 \\ 0 & 1 & 0 \\ 0 & 0 & e^{-100s} \end{bmatrix} \quad (A1)$$

so that the resulting process transfer function matrix becomes

$$G_p^{new}(s) = \begin{bmatrix} \frac{4.05e^{-300s}}{50s+1} & \frac{1.77e^{-300s}}{60s+1} & \frac{5.88e^{-350s}}{50s+1} \\ \frac{5.39e^{-300s}}{50s+1} & \frac{5.72e^{-300s}}{60s+1} & \frac{6.9e^{-300s}}{40s+1} \end{bmatrix}. \quad (A2)$$

Thus, based on $G_p^{new}(s)$ all the decouplers including D_{23} and D_{21} can be obtained in realizable form. But, the addition of the delay matrix to the original process results in the closed-loop performance delayed further, which is not desirable in the practical industry. Hence, if the time delay required for the addition is very small compared to the original delay then the delay matrix can be added at the cost of delayed performance. However, if the delay matrix required is large as in this example, it is not recommended to use the additional delay matrix because of the problems encountered by time delays in the practical industries.

Appendix B

The SIMC method proposed by Skogestad [16] is based on the original IMC method in which he modified the choice of choosing the IMC filter constant as equal to the time delay. Also, the integral time is modified for better disturbance attenuation. The final tuning relations for a FOPTD model are as follows.

$$\text{Process model } (G_m) = \frac{ke^{-qs}}{ts+1},$$

$K_c = \frac{1}{k} \frac{t}{t_c + q}$, $t_i = \min(t, 4(t_c + q))$ in which t_c is the tuning parameter which according to Skogestad [16] can be considered as equal to time delay (q)

Abbreviations

- BRG Block relative gain array
- FOPTD First-order plus time delay
- ISE Integral of square error
- IMC Internal model control
- LS Least square

MIMO	Multi input multi output
SISO	Single input single output
SIMC	Simplified internal model control
SOPTD	Second-order plus time delay
PRC	Process reaction curve

Nomenclature

G_c	Transfer function matrix of controller
P	Transfer function matrix of decoupled process with time delay
P_m	Transfer function matrix of decoupled process model without time delay
G_p	Transfer function matrix of process with time delay
K_c	Proportional gain of the controller
y_{r1}	Set point for output variable 1
y_{r2}	Set point for output variable 2
u_i	Manipulated variables where $i = 1, 2, 3, 4, \dots$
y_i	Controlled variables where $i = 1, 2, \dots$

Greek letters

t_1	Time constant of the decoupled process model
t_2	Time constant of the process decoupled process model
t_{cl}	Tuning parameter
t_c	Tuning parameter in the controller design for SIMC method for uncompensated system
t_s	Tuning parameter in the controller design for IMC method for compensated system
t_I	Integral time constant of the controller
t_D	Derivative time constant of the controller
t_F	Filter time constant
Δ_A	Additive uncertainty
Δ_I	Input multiplicative uncertainty
Δ_o	Output multiplicative uncertainty